Madencilik - Mining, 2022, 61(3), 127-134

BİLİMSEL MADENCİLİK DERGİSİ
SCIENTIFIC MINING JOURNAL

TMMOB Maden Mühendisleri Odası Yayını / The Publication of the Chamber of Mining Engineers of Turkey

www.mining.org.tr

Original Research / Orijinal Araştırma

Turbulence models and simulation method in the CFD simulation of 75-mm hydrocyclone

75 mm hidrosiklonun CFD simülasyonunda türbülans modelleri ve simülasyon yöntemi

Song Gun Kang[a,*], Kwang Chol Kim[a,**], Sok Chol Ryom[a,***], Jin Hyok Ri[b,****]

[a] *Department of Mining Engineering, Kim Chaek University of Technology, Pyongyang, DPR Korea*
[b] *Department of Chemistry, University of Science, Pyongyang, DPR Korea*

*Geliş-Received: 15 Temmuz - July 2021 * Kabul - Accepted: 10 Şubat - February 2022*

A B S T R A C T

In this paper, an effective method for the classification process simulation in 75mm hydrocyclone is considered. The simulation results and computational time are compared using Reynolds stress model (RSM) and different large eddy simulation (LES) subgrid-scale models as turbulence models. The Lagrangian discrete phase model (DPM) is used to simulate the classification process of particles. As the experimental result for comparison of simulation results, Hsieh's experimental data are used. When the different LES subgrid-scale models are used, the solution converges stably by various solution convergence methods without increasing the grid numbers or reducing the size of time steps than RSM model. As a result, it is confirmed that when an appropriate simulation method is applied with the LES-WMLES S-Omega model, more accurate axial water flow velocity distribution and particle classification simulation results can be obtained at a computational cost similar to that of using the RSM model. By drawing the partition curve, it is possible to select a hydrocyclone with low bypassing of fine particles and high classification efficiency.

Keywords: *Hydrocyclone, Turbulence model, Computational cost, Particle classification, CFD simulation*

Introduction

The hydrocyclone for classification has been studied by many researchers historically due to its simple structure, easy installation and manufacturing, and good separation efficiency for fine particles. Here, “good separation efficiency” means that the hydrocyclone has better separation efficiency than the mechanical classifier in classifying fine particles that are usually smaller than 74 microns. However, the bypass of the fine material to the underflow is a significant problem in cyclone classification. Although this phenomenon cannot be completely eliminated in the hydrocyclone, it can be reduced and the separation efficiency can be increased. For this purpose, it is important to accurately determine the operating and geometric factors of the hydrocyclone.

In general, the problem of selecting one hydrocyclone with the highest classification efficiency among hydrocyclones with different structures and geometric dimensions that satisfies the user's requirements can be proceeded in two ways, one is an experiment and the other is a computer simulation. Here, when the simulation result is as realistic as the experiment result, the method of selecting a hydrocyclone by simulation is economically significant.

Today, a study on the simulation of the classification process in the hydrocyclone based on computational fluid dynamics (CFD) is widely conducted, and realistic research results have been published by many researchers. The most widely used research data as verification data for the results of the water-air two-phase simulation and the classification process simulation in the hydrocyclone with dilute slurry is Hsieh's experimental data published in 1988 (Hsieh, 1988).

The simulation stage of the classification process in the hydrocyclone can be divided into two stages. The first step is to proceed with the water-air two-phase simulation to obtain a stable air column and fluid flow field in the hydrocyclone. The second step conducts a multiphase flow simulation to evaluate the classification efficiency, using the flow field in the first step as an initial condition.

The simulation method of the classification process in the hydrocyclone can also be divided into two. One is to proceed with the steady solution first to obtain a flow field, and then combine the unsteady solution to simulate the classification process (Brennan et al., 2007; Ghadirian et al., 2013; Li et al., 2018). This method cannot consider the detailed changes over time for the change

* Corresponding author / Sorumlu yazar: jiangchenggenfstar@163.com https://orcid.org/0000-0003-1237-3712
** kwangchok_kim@163.com https://orcid.org/0000-0002-6270-0702
*** sokchol_ryom@163.com https://orcid.org/0000-0003-1838-4148
**** jinhyok_ri@163.com https://orcid.org/0000-0002-4725-8856

https://doi.org/10.30797/madencilik.971842

of the flow field, especially the formation of the air column, in the hydrocyclone, but the classification result can be obtained. The other is to solve unsteady conditions over time from the beginning just like in reality (Narasimha et al., 2012; Ghodrat et al., 2016; Vakamalla et al., 2016; Jiang et al., 2019; Ye et al., 2019; Padhi et al., 2020).

The selection of the turbulence model is important in simulation of the hydrocyclone. The turbulence models giving the simulation results similar to the experimental values are RSM-LPS, RSM-QPS (Kuang et al., 2012; Silva et al., 2014; Cui et al., 2017; Zhang et al., 2017; Perez et al., 2018; Mangadoddy et al., 2019) and LES-Smagorinsky-Lilly (Delgadillo and Rajamani, 2007; Delgadillo and Rajamani, 2009; Wang et al., 2015; Padhi et al., 2019; Vakamalla and Mangadoddy, 2019; Padhi et al., 2020) models. The simulation method by the RSM model is the best choice for coarser meshes. It is evaluated that the RSM-VOF model is more accurate in prediction of the pressure drop and the fluid split ratio into the spigot, and that the LES-VOF model is more accurate in prediction of the tangential velocity distribution (Ghodrat et al., 2016). In the tangential velocity distribution prediction, it is consistent with all the literatures that the prediction result by the LES-VOF model is more accurate than the prediction result by the RSM-VOF model. The simulation results predicted by the RSM model and the LES model do not agree numerically, but all fall within the engineering tolerance. The coarser mesh may be used in the simulation using the RSM model, so the computational cost is less than that of the simulation using LES model. The simulation result by the LES model is accurate (Delgadillo and Rajamani, 2005; Delgadillo, 2006), but the computational cost is higher and the solve convergence is poor (Li et al., 2018; Perez et al., 2018; Jiang et al., 2019; Ye et al., 2019).

Since the hydrocyclone is the equipment that is widely used in various fields, it is practical only to obtain simulation results within a certain time by using a personal computer. Therefore, in the simulation of the classification process of the hydrocyclone, both the accuracy of the simulation and the calculation cost are very important. This problem can be solved by using the LES model and applying a simulation method that allows the solution to converge stably and quickly as the RSM model. There are four subgrid-scale models, the Smagorinsky-Lilly model, the WALE model, the WM-LES, and the WMLES S-Omega model, in the LES model. In the literature, there is no mention of the comprehensive simulation results for the four subgrid-scale models of the LES model.

Therefore, in this paper, authors try to establish a simulation method with low computational cost and high simulation accuracy by selecting the subgrid-scale models of the LES model well and applying the solution convergence methods that can increase the convergence safety.

1. Simulation

The RSM turbulence model, VOF and DPM models, which have been frequently mentioned in the literature, are not described again here.

1.1. Mathematical model

The governing equations employed for LES are obtained by filtering the time-dependent Navier-Stokes equations in physical space. The filtered Navier-stocks equation has the following form: (ρ: Density, kg/m^3, u: Fluid velocity, m/s, t: Time ,s, x: Cartesian coordinate):

$$\frac{\partial}{\partial t}(\rho\bar{u}_i) + \frac{\partial}{\partial x_j}(\rho\bar{u}_i\bar{u}_j) = \frac{\partial}{\partial x_j}(\sigma_{ij}) - \frac{\partial\bar{p}}{\partial x_i} - \frac{\partial\tau_{ij}}{\partial x_j} \quad (1)$$

where is the stress tensor due to molecular viscosity defined by

$$\sigma_{ij} \equiv \left[\mu\left(\frac{\partial u_i}{\partial x_j} + \frac{\partial u_j}{\partial x_i}\right)\right] - \frac{2}{3}\mu\frac{\partial u_l}{\partial x_l}\delta_{ij} \quad (2)$$

and τ_{ij} is the subgrid-scale stress defined by

$$\tau_{ij} \equiv \rho\overline{u_i u_j} - \rho\bar{u}_i\bar{u}_j \quad (3)$$

The subgrid-scale turbulence models in ANSYS Fluent employ the Boussinesq hypothesis, computing subgrid-scale turbulent stresses from

$$\tau_{ij} - \frac{1}{3}\tau_{kk}\delta_{ij} = -2\mu_t\bar{S}_{ij} \quad (4)$$

where is the subgrid-scale turbulent viscosity.

The isotropic part of the subgrid-scale stresses is not modeled, but added to the filtered static pressure term.

$\bar{S}_{ij}$ is the strain rate tensor for the resolved scale defined by

$$\bar{S}_{ij} \equiv \frac{1}{2}\left(\frac{\partial\bar{u}_i}{\partial x_j} + \frac{\partial\bar{u}_j}{\partial x_i}\right) \quad (5)$$

ANSYS Fluent offers the following models for .

1.1.1. Smagorinsky-Lilly Model

In the Smagorinsky-Lilly model, the turbulent viscosity is modeled as follows:

$$\mu_t = \rho L_S^2\left|\bar{S}_{ij}\right| \quad (6)$$

$$L_S = \min(kd, C_S\Delta) \quad (7)$$

$$\Delta = V^{1/3} \quad (8)$$

where L_s is the mixing length for subgrid scales, k=0.1 is the von Karman constant, d is the distance to the closest wall, C_s is Smagorinski constant, Δ is the grid size and V is the volume of the computational cell.

1.1.2. Wall-Adapting Local Eddy-Viscosity (WALE) Model

In the WALE model, the turbulent viscosity is modeled as follows:

$$\mu_t = \rho L_S^2\frac{(S_{ij}^d S_{ij}^d)^{3/2}}{(\bar{S}_{ij}\bar{S}_{ij})^{5/2} + (S_{ij}^d S_{ij}^d)^{5/4}} \quad (9)$$

$$L_S = min(kd, C_w V^{1/3}) \quad (10)$$

$$S_{ij}^d = \frac{1}{2}\left(\bar{g}_{ij}^2 + \bar{g}_{ji}^2\right) - \frac{1}{3}\delta_{ij}\bar{g}_{kk}^2 \quad (11)$$

$$\bar{g}_{ij} = \frac{\partial\bar{u}_i}{\partial x_j} \quad (12)$$

where C_w is the WALE constant. The rest of the notation is the same as for the Smagorinsky-Lilly model.

1.1.3. Algebraic Wall-Modeled LES (WMLES) Model

In the WMLES model, the turbulent viscosity is modeled as follows:

$$\mu_t = min[(kd_w)^2, \left(C_{S_{mag}}\Delta\right)^2] \cdot \rho \cdot S \cdot \{1 - exp[-(y^+/25)^3]\} \quad (13)$$

where d_w is the wall distance, S is the strain rate, k=0.4187 and C_{smag} are constants, y^+ is the normal to wall inner scaling, ρ is the fluid density, and Δ is the grid size.

$$\Delta = min(max(C_w \cdot d_w; C_w \cdot h_{max}, h_{wn}); h_{max}) \quad (14)$$

where h_{max} is the maximum edge length for a rectilinear hexahedral cell, $h_{wn\ mag}$ is the wall-normal grid spacing, and C_W is a constant.

1.1.4. Algebraic WMLES S-Omega Model

In the WMLE S-Omega model, the turbulent viscosity is modeled as follows:

$$\mu_t = min\left[(kd_w)^2, \left(C_{S_{mag}}\Delta\right)^2 \cdot \rho \cdot (|S - \Omega|) \cdot \{1 - exp[-(y^+/25)^3]\}\right] \quad (15)$$

where Ώ is the vorticity magnitude. The rest of the notation is the same as for the WMLES model.

1.2. Simulation condition

Figure 1 shows the geometric shape and mesh model of Hsieh's 75-mm hydrocyclone used in the simulation. A geometric model is created in Solidworks program and grid formation is performed in ICEM CFD program. All dimensions indicated in Figure 1 are in mm. The mesh is made of hexahedral cells, and the gird is made finer in the vicinity of the wall and at the inlet and outlets. In addition, the grid is made fine, as descending from the cone part to the spigot.

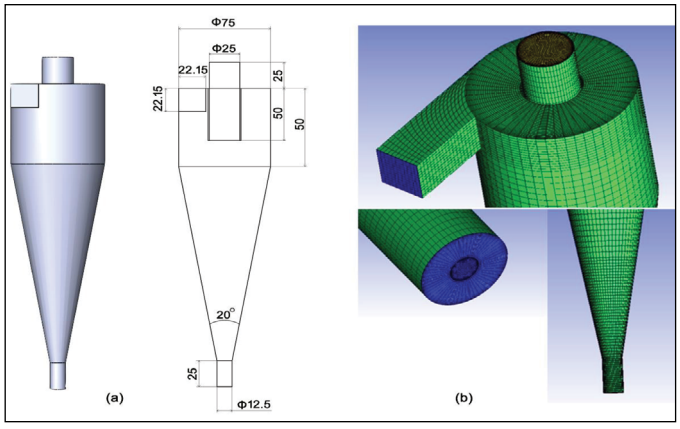

Figure 1. *Geometrical shape and mesh model. (a) geometrical shape. (b) mesh model.*

In the simulation, the grid numbers of 162711 cells and 305377 cells are used.

The classification process simulation is conducted in the Fluent program of ANSYS 2020 R1.

Water is set as the primary phase and air is set as the secondary phase.

As the boundary conditions, velocity inlet and pressure outlet conditions are used. Considering Hsieh's No 1 test conditions, the inlet velocity is set to 2.275 m/s. The inlet turbulent intensity is set to 10%. It is assumed that no air enters through the inlet. The air backflow volume fraction is set to 1 in the spigot and the vortex finder.

The residual values for all solution variables are set to 1×10^{-4} -1×10^{-5}.

The fixed time step size is set by the following calculation. Courant number is calculated as follows:

$$C = \frac{U \cdot \Delta t}{\Delta h} \quad (16)$$

where U indicates the flow velocity, Δt is a representative time step of the simulation and Δh is the characteristic size of the mesh cell.

The Courant number must be less than 2.5 in the hydrocyclone simulation, so that the linear stability of the numerical calculation can be maintained. If the number of grid cells is 162711 cells, the minimum length of the cell is 1.9808×10^{-4} m. Calculating with the current simulation values, $=2.1767\times10^{-4}$ s. Therefore, the time step size is fixed at 1×10^{-4} s.

For the research purpose of this paper, the time step sizes are fixed to 1×10^{-4} s for both the RSM model and the LES model.

The particles used for the particle classification are determined as shown in Table 1 based on Hsieh's No 7 experiment. All particles are assumed to be spherical and enter the inlet at the same speed as water. The density of limestone particles is 2700 kg/m^3.

Table 1. *Particles used for simulation*

Particle size, microns	Mass Flow rate, kg/s	Particle size, microns	Mass Flow rate, kg/s
35.5	0.006869	4.43	0.0039055
25.1	0.0102174	3.13	0.0024007
17.74	0.0113373	2.11	0.0017575
12.55	0.0074951	1.31	0.0015909
8.87	0.0052264	0.82	0.001051
6.7	0.0050082	0.53	0.0005743

1.3. Simulation method

The unsteady simulation with a fixed time step is carried out to obtain a fluid flow yield in which a stable air column is formed. The VOF model is used as a multiphase model for air column formation. As turbulence models, RSM-LPS, LES-Smagorinsky-Lilly, LES-WALE, LES-WMLES, and LES-WMLES S-Omega models are used, respectively. The parameters of the turbulence model use the default values of the program without change. Implicit formulation is selected in the volume fraction parameters of the multiphase model.

As the solution method, the SIMPLE pressure-velocity coupling algorithm is used. The discretizations of pressure and volume fraction are respectively set as PRESTO, Modified HRIC, and all other items are set as QUICK.

The following solution convergence method is applied to the LES models. The under-relaxation factors are 0.7-0.8 (default 0.3) for pressure, 0.3-0.2 (default 0.7) for momentum and default values for the rest. The residual values of the solution variables are initially set to 1×10^{-4}, and when the solution stays at a certain limit and no longer converges, the solutions are converged by setting

them to 1×10^{-5}. If the solution diverges after a certain period of time, the 1st-order term and the higher-order term are blended to continue the simulation and 1st-order to higher-order blending factor is set to 0.95-0.97. The reason why the relaxation factors are changed for pressure and moment is because the solution does not converge properly with the default values in the simulation using the LES model.

Solution convergence is determined with the following way. After a stable air column is formed, the difference in mass flow rates between the inlet and outlets is calculated. The mass flow rates at the inlet and outlets are time-averaged values over 1s (10000 iteration numbers) for instantaneous values. If this time-averaged mass flow difference value is less than 1% of the inlet value and remains stability for more than 1 s (10000 iteration numbers), the solution is judged to have converged.

After the fluid simulation reaches a steady state, the DPM is used to simulate the particle classification. Since the current simulation is for dilute slurry, the uncoupled DPM and the steady tracking are used to track the movement of particles to the spigot.

2. Result and discussion

2.1. Choice of mesh

For choice of mesh, two-phase simulation has been performed for 162711 cells and 305377 cells with the RSM-LPS model. Based on previous literature studies, the authors do not feel the need to conduct the choice test for 160000 cells or less.

Table 2. *Mass balance and water split ratio and the experiment of Hsieh*

Ülke	Mass Flow rate , kg/s			Water split Ratio, %	Computational time, hours
	Feed	Overflow	Underflow		
Experiment	1.1165	1.062	0.0545	95.12	-
162711 cells	1.1142	1.0266	0.0876	92.14	102
305377 cells	1.1142	1.0264	0.0878	92.12	125

Table 2 shows the water split ratio to overflow at simulation time 4.2 s, which is similar in coarse and fine meshes. The solution starts to enter a state of complete convergence from 3.2 s. As shown in Table 2, there is no significant difference between the experimental and simulation results for water split to overflow. Also, the simulation results for the water split in the coarse mesh and the fine mesh simulation are similar. Therefore, in terms of water split ratio and computational time, it is more reasonable to select the coarse mesh.

Figure 2 shows the axial and tangential velocities on the 0-180^o plane and 90- 270^o plane at the 60 mm from the top of cyclone as in Hsieh's experimental results. As shown in the velocity distribution in Figure 2, the tendency and number values of the velocity distribution according to the radius are similar in the simulation results of fine and coarse mesh. When the mesh is 305377 cells, the relative error value between the experimental and simulation results in the velocity distribution is less than 10%, so authors do not feel the need to proceed with the simulation for a finer mesh.

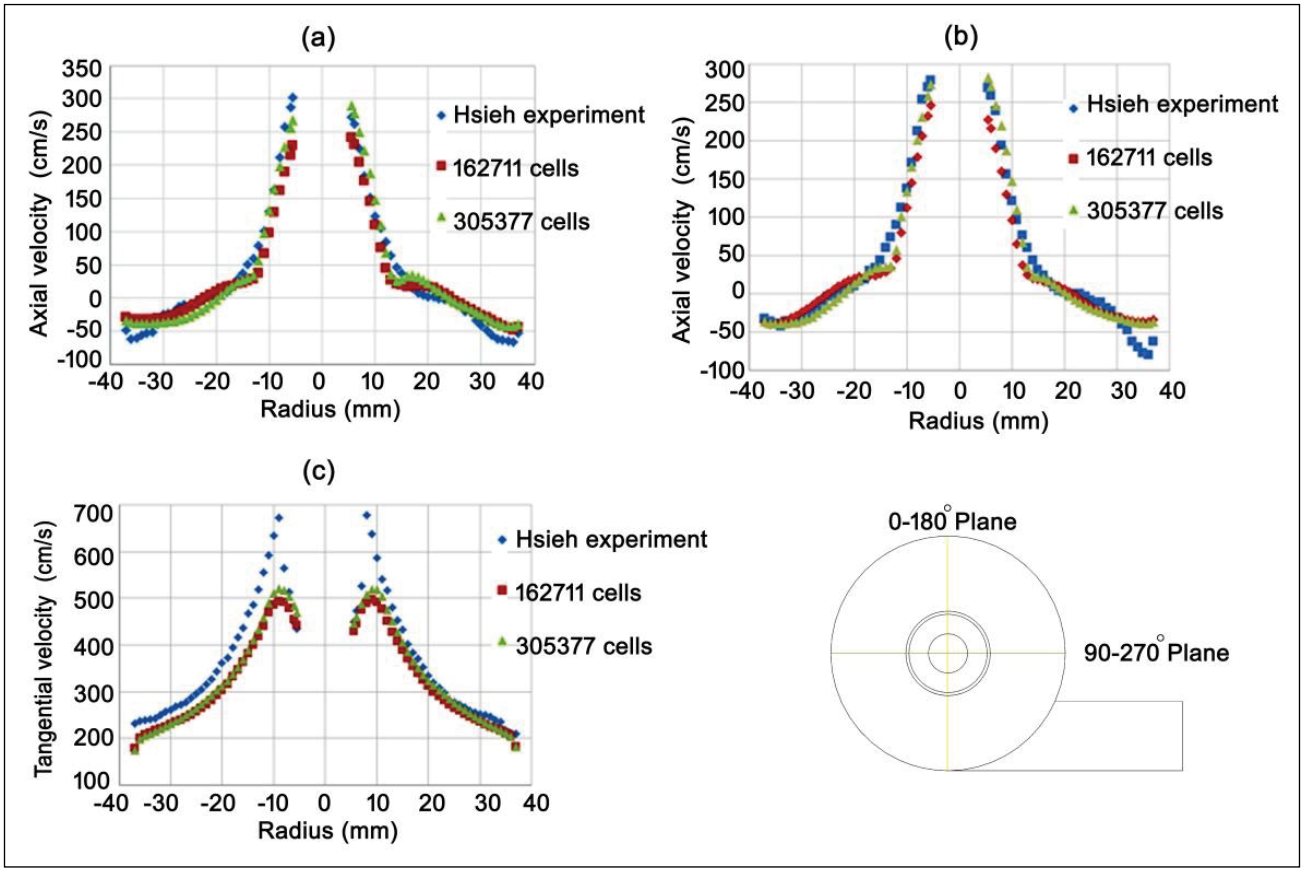

Figure 2. *Axial velocities on (a) 0-180^o plane, (b) 90-270^o plane, and (c) tangential velocities on 0-180^o plane at 60mm from the top of cyclone in mesh choice simulation*

Therefore, the mesh of 162711 cells is reasonable in simulation of classification process of 75-mm hydrocyclone with dilute slurry.

2.2. Evaluation on the turbulence models

Two-phase and classification process simulations are conducted using RSM-LPS, LES- Smagorinsky-Lilly, LES-WALE, LES-WMLES, and LES-WMLE S Omega turbulence models, and the simulation results are compared with Hsieh's experimental results. The RSM model and the LES model differ greatly in the convergence stability of simulation. Considering the simulation process, in the simulation by the RSM model, the solution stably enters the convergence state after a certain period of time. However, in the simulation by the LES model, the solution does not easily enter the convergence state even after a certain period of time.

In the simulation using the LES-WALE model and the LES-WMLES model, even though the solution convergence methods are applied, the solution does not converge even after the computational time of 160 hours. Thus, they are excluded from the comparison of simulation results because the purpose of this paper is simulation accuracy and computational cost.

Table 3 shows the water split ratio and computational time after the solution by the water-air two-phase simulation reaches a stable convergence state. These simulation results are results when the simulation times are 4.2 s for RSM-LPS model, 5.5 s for LES-Smagorinsky-Lilly model and 4.5 s for LES-WMLES S Omega model, respectively. Where, the water split ratios to overflow are calculated the mass flow rate values to feed and overflow in experiment and simulations. In the experiment, the water split ratio to overflow is 95.12%, and in the simulation using the RSM-LPS, LES-Smagorinsky-Lilly, and LES-WMLES S Omega models, the water split ratios are 92.14%, 88.26%, and 92.18%, respectively. As can be seen from these results, the simulation result most similar to the experimental value is obtained from simulation using the LES-WMLES S Omega model. The computational time is also the smallest in the simulation using the LES-WMLES S Omega model, 96 hours. Therefore, the simulation by the LES-WMLES S Omega model is the most accurate for predicting water split ratio and the smallest in computational time.

In the simulation results by the different turbulence models, the distribution of the axial and tangential velocities of water at the 60 mm from the top of cyclone is shown in Figure 3.

Table 3. *Water split ratio and computational time*

Ülke	Mass Flow rate, kg/s			Water split Ratio, %	Computational time, hours
	Feed	Overflow	Underflow		
Experiment	1.1165	1.062	0.0545	95.12	-
RSM-LPS	1.1142	1.0266	0.0876	92.14	102
LES-Smagorinsky-Lilly	1.1078	0.9777	0.1301	88.26	163
LES-WMLES S Omega	1.1142	1.0271	0.0871	92.18	96

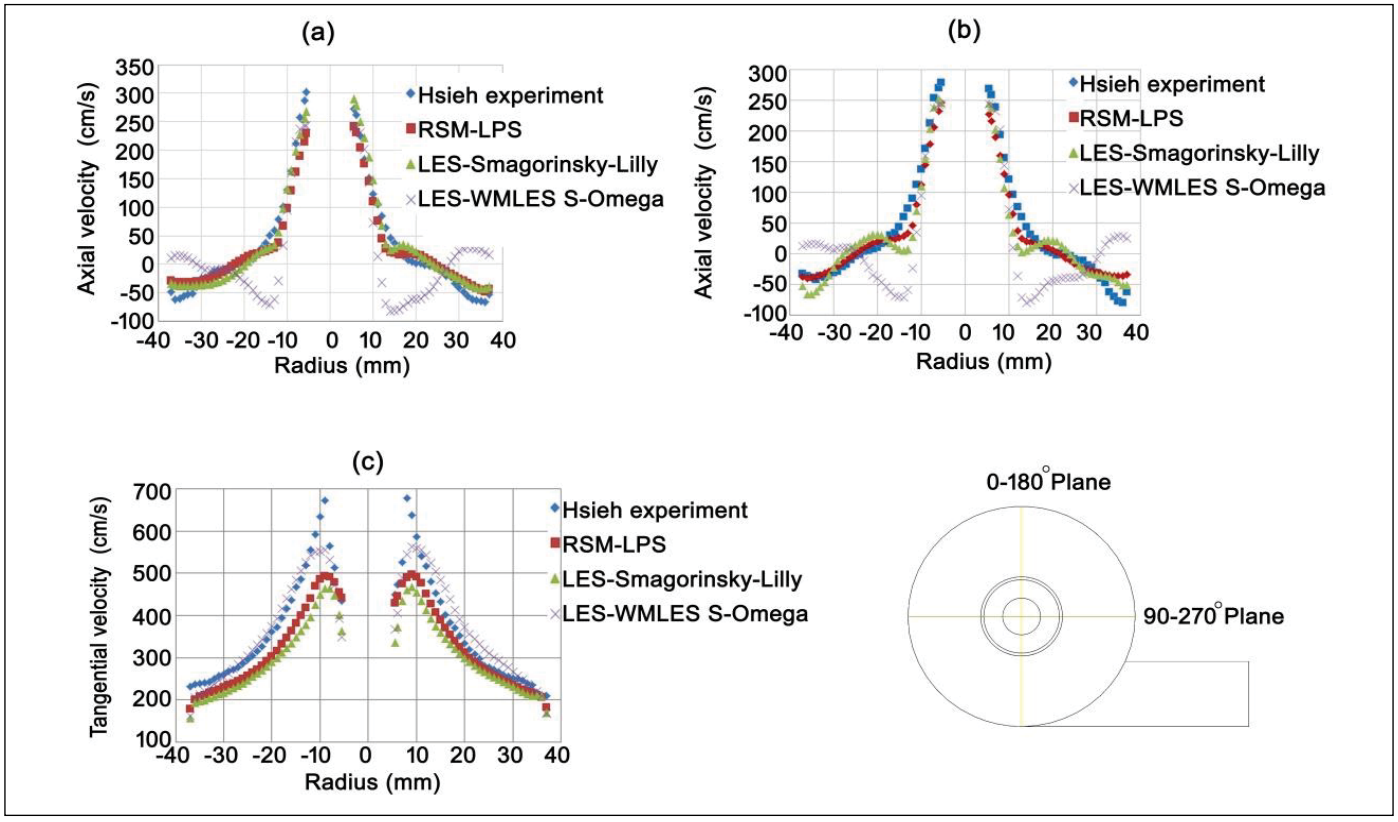

Figure 3. *Axial velocities on (a) 0-180° plane; (b) 90-270° plane; (c) tangential velocities on 0-180° plane at 60mm from the top of cyclone in different turbulence model simulation*

As shown in Figure 3, the accuracy order for axial velocity distribution prediction is RSM-LPS, LES-Smagorinsky-Lilly, and LES-WMLES S-Omega models. However, the accuracy order for tangential velocity distribution prediction is the LES-WMLES S-Omega, RSM-LPS, and LES-Smagorinsky models. In particular, the relative error between the mathematical average of the predicted values of the tangential velocity distribution by the LES-WMLES S-Omega model and the mathematical average of the experimental values is 0.7%, and the prediction of the tangential velocity distribution by this model is very accurate.

As shown in Figure 4, the shape and size of the air column in a stable state are similar to each other in the simulation using the three models. Considering the formation state of the air column, air enters from the outside through the vortex finder and the spigot at the same time and collides at a certain position. At this time, since the velocity of the air coming in through the spigot is faster than the velocity of the air coming in through the vortex finder, the air goes out to the vortex finder together. This principle is clear by considering the axial velocity vector diagram as shown in Figure 5. The turbulence model order in which this principle is most clearly expressed is the RSM-LPS, LES-Smagorinsky, and LES-WMLES S-Omega models.

The computational time of the two-phase simulation is 96 hours for the LES-WMLES S-Omega model, 102 hours for the RSM-LPS model, and 163 hours for the LES-Smagorinsky-Lilly model.

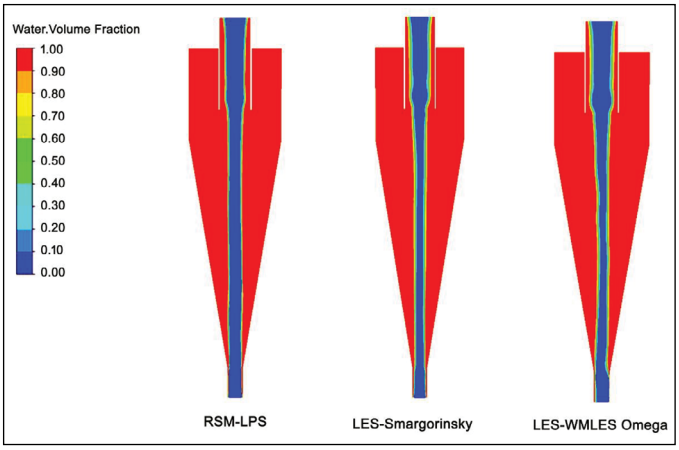

Figure 4. *Shape of air column in the stable state*

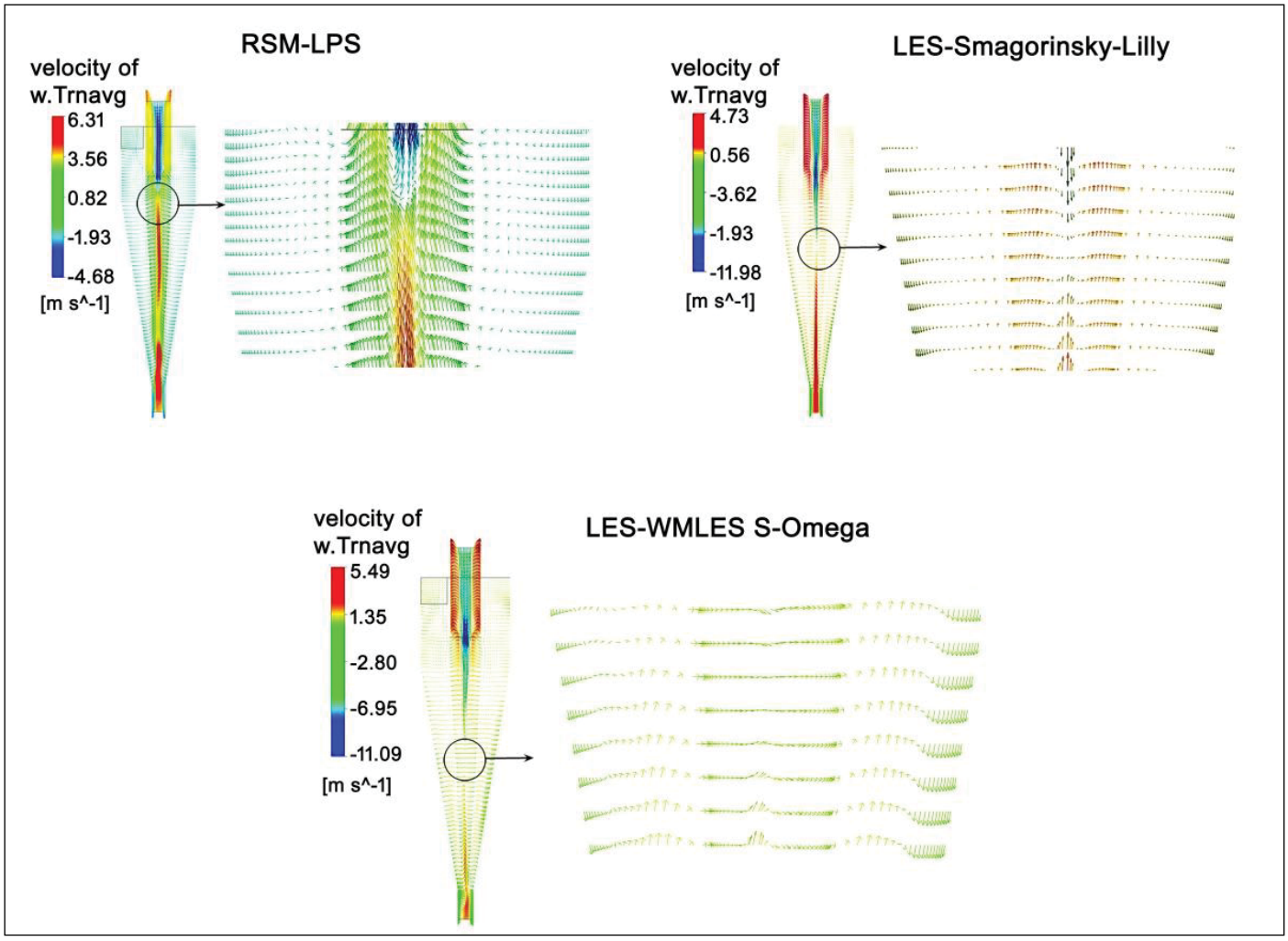

Figure 5. *Axial velocity vector diagram.*

Based on the results of the two-phase simulation of the different turbulence models, the simulation for the particle classification of Hsieh's No 7 experiment is conducted with the DPM model and compared with the experiment results. The simulation result for the particle classification is shown in Figure 6. Figure 6 is the corrected partition curves. The purpose of research is the establishment of simulation method, the simulation which is the nearest with experiment result is the best correct simulation. The best correct method among the simulation methods is selected by comparing the correlation coefficient and the corrected cut-size between the experimental values and the simulation values. With recovery to underflow for each particle, correlation coefficients of simulation values on experimental values are calculated. The correlation coefficient values are 0.997 for the LES-WMLES S-Omega model, 0.994 for the RSM-LPS model, and 0.977 for the LES-Smagorinsky-Lilly model, respectively. The corrected cut-size is 18.15 microns in Hsieh's experiment, 16.76 microns for the RSM-LPS model, 16.5 microns for the LES-Smagorinsky-Lilly model, and 18.11 microns for the LES-WMLES S-Omega model. As a result, the simulation result by the LES-WMLES S-Omega model is the most accurate in the prediction for the particle classification of the Hsieh's 75-mm hydrocyclone.

The following facts can be found form the simulation results of the water velocity distribution by the water-air two-phase simulation and the classification process simulation results of particles based thereon. Among the axial and tangential velocities of water in the hydrocyclone, the velocity that greatly affects the classification result of the particles is the tangential velocity. This is because the tangential velocity distribution is the most accurate, the result of the axial velocity distribution simulation is relatively inaccurate, and the particle classification simulation result is the most accurate than other models in the simulation results by the LES- WMLES S-Omega turbulence model.

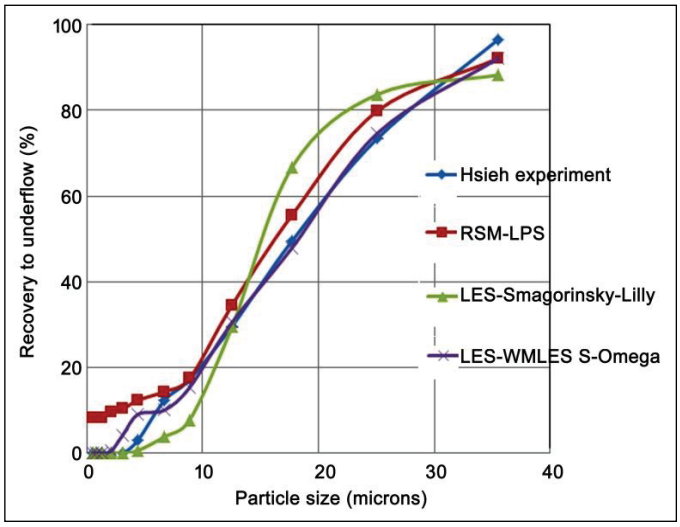

Figure 6. *Particle classification using the different turbulence models*

The tangential and axial velocities in the hydrocyclone are the velocities that occur under the action of centrifugal and gravitational forces. The tangential velocity is mainly influenced by centrifugal force, and the axial velocity is mainly influenced by gravity. Eventually, under Hsieh's hydrocyclone test conditions, it is found that fine particles of less than 35 microns are mainly classified under the influence of centrifugal forces.

Conclusions

In the simulation of the classification process of the Hsieh's 75-mm hydrocyclone for dilute slurry with a mass concentration of less than 10%, LES- WMLES S-Omega model should be used to obtain more accurate tangential velocities and particle classification simulation results. In this case, the computational cost of the simulation is similar with using the RSM model. The set of residual values of the solution variables should be changed from 10-4 to 10-5 during the solution, the 1st-order term and the higher-order term should be blended for the convergence of solution. The under-relaxation factors are 0.7-0.8 (default 0.3) for pressure, 0.3-0.2 (default 0.7) for momentum in LES model simulation.

It is sufficient to use about 160,000 hexahedral cells to simulate the classification process in the Hsieh's 75-mm hydrocyclone for dilute slurry with a mass concentration of 10% or less.

In the hydrocyclone simulation, the axial velocity distribution of the medium mainly affects the accurate simulation results for the formation of the air column, and the tangential velocity distribution mainly affects the accurate simulation results for the particle classification.

This simulation method can be used to obtain the accurate simulation results within a reasonable time on a personal computer. When an accurate simulation method is established, the simulation can be carried out by changing the operation and geometric parameters of the hydrocyclone based on it. The smaller the partition of fine particles bypassing classification in the hydrocyclone, which proceeds with the classification for the same cut-size, the higher the classification efficiency. By calculating the partitions for each particles to underflow from the simulation results and drawing the partition curve, it is possible to select a hydrocyclone with low bypassing of fine particles and high classification efficiency.

References

Brennan, M.S., Narasimha, M., Holtham, P.N. 2007. Multiphase modelling of hydrocyclones - prediction of cut-size. Minerals Engineering 20, 395-406. doi:10.1016/j.mineng.2006.10.010.

Cui, B., Zhang, C., Wei, D., Lu, S., Feng, Y. 2017. Effects of feed size distribution on separation performance of hydrocyclones with different vortex finder diameters. Powder Technology 322, 114-123. doi:10.1016/j.powtec.2017.09.010.

Delgadillo, J.A., Rajamani, R.K. 2005. A comparative study of three turbulence - closure models for the hydrocyclone problem. International journal of mineral processing 77(4), 217-230. doi:10.1016/j.minpro.2005.06.007.

Delgadillo, J.A. 2006. Modelling of 75- and 250-mm hydrocyclones and exploration of novel designs using computational fluid dynamics Ph.D. thesis. Utah: The University of Utah.

Delgadillo, J.A., Rajamani, R.K. 2007. Exploration of hydrocyclone designs using computational fluid dynamics. International Journal of Mineral Processing 84, 252-261. doi:10.1016/j.minpro.2006.07.014.

Delgadillo, J.A., Rajamani, R.K. 2009. Computational fluid dynamics prediction of the air-core in hydrocyclones. International Journal of Computational Fluid Dynamics 23(2), 189-197. doi:10.1080/10618560902724893.

Ghadirian, M., Hayes, R.E., Mmbaga, J., Afacan, A., Xu, Z. 2013. On the simulation of hydrocyclones using CFD. The Canadian Journal of Chemical Engineering 91(5), 950-958. doi:10.1002/cjce.21705.

Ghodrat, M., Qi, Z., Kuang, S.B., Ji, L., Yu, A.B. 2016. Computational investigation of the effect of particle density on the multiphase flows and performance of hydrocyclone. Minerals Engineering 90, 55-69. doi:10.1016/j.mineng.2016.03.017.

Hsieh, K.T. 1988. Phenomenological model of the hydrocyclone. Ph.D. thesis. Utah: The University of Utah.

Jiang, L., Liu, P., Zhang, Y., Yang, X., Wang, H., Gui, X. 2019. Design boundary layer structure for improving the particle separation performance of a hydrocyclone. Powder Technology 350, 1-14. doi:10.1016/j.powtec.2019.03.026.

Kuang, S.B., Chu, K.W., Yu, A.B., Vince, A. 2012. Numerical study of liquidgas-solid flow in classifying hydrocyclones: Effect of feed solids concentration. Minerals Engineering 31, 17-31. doi:10.1016/j.mineng.2012.01.003.

Li, Y., Liu, C., Zhang, T., Li, D., Zheng, L. 2018. Experimental and Numerical Study of a Hydrocyclone with the Modification of Geometrical Structure. The Canadian Journal of Chemical Engineering 96, 2638-2649. doi:10.1002/cjce.23206.

Mangadoddy, N., Vakamalla, T.R., Kumar, M., Mainza, A. 2019. Computational modelling of particle-fluid dynamics in comminution and classification: a review. Mineral Processing and Extractive Metallurgy 129(2), 145-156. doi:10.1080/25726641.2019.1708657.

Narasimha, M., Brennan, M., Holtham, P.N. 2012. CFD modeling of hydrocyclones: Prediction of particle size segregation. Minerals Engineering 39, 173-183.

Padhi, M., Mangadoddy, N., Sreenivas, T., Vakamalla, T.R., Mainza, A.N. 2019. Study on multi-component particle behaviour in a hydrocyclone classifier using experimental and computational fluid dynamics techniques. Separation and Purification Technology 229, 115698. doi:10.1016/j.seppur.2019.115698.

Padhi, M., Kumar, M., Mangadoddy, N. 2020. Understanding the bicomponent particle separation mechanism in a hydrocyclone using a computational fluid dynamics model. Industrial & Engineering Chemistry Research 59(25), 11621- 11644. doi:10.1021/acs.iecr.9b06747.

Perez, D., Cornejo, P., Rodriguez, C., Concha, F. 2018. Transition from spray to roping in hydrocyclones. Minerals Engineering 123, 71-84. doi:10.1016/j.mineng.2018.04.008.

Silva, D.O., Vieira, L.G.M., Barrozo, M.A.S. 2014. Optimization of design and performance of solid-liquid separators: A thickener hydrocyclone. Chemical Engineering & Technology 38(2), 319-326. doi:10.1002/ceat.201300464.

Vakamalla, T.R., Koruprolu, V.B., Arugonda, R., Mangadoddy, N. 2016. Development of novel hydrocyclone designs for improved fines classification Using multiphase CFD model. Separation and Purification Technology 175, 481-497. doi:10.1016/j.seppur.2016.10.026.

Vakamalla, T.R., Mangadoddy, N. 2019. The dynamic behaviour of a large-scale 250-mm hydrocyclone: A CFD study. Asia-Pacific Journal of Chemical Engineering 14(2), e2287. doi: 10.1002/apj.2287.

Wang, C., Ji, C., Zou, J. 2015. Simulation and experiment on transitional behaviours of multiphase flow in a hydrocyclone. The Canadian Journal of Chemical Engineering 93, 1802-1811. doi:10.1002/cjce.22274.

Ye, J., Xu, Y., Song, X., Yu, J. 2019. Novel conical section design for ultra-fine particles classification by a hydrocyclone. Chemical Engineering Research and Design 144, 135-149. doi:10.1016/j.cherd.2019.02.006.

Zhang, Y., Cai, P., Jiang, F., Dong, K., Jiang, Y., Wang, B. 2017. Understanding the separation of particles in a hydrocyclone by force analysis. Powder Technology 322, 471-489. doi:10.1016/j.powtec.2017.09.031.